7 General Concepts on Radioguided Sentinel Lymph Node Biopsy: Preoperative Imaging, Intraoperative Gamma-Probe Guidance, Intraoperative Imaging, and Multimodality Imaging

Federica Orsini, Federica Guidoccio, Sergi Vidal-Sicart, Renato A. Valdés Olmos, and Giuliano Mariani

7.1 Introduction

Lymphoscintigraphy is an essential component for radioguided sentinel lymph node biopsy (SLNB), which is now routinely employed in clinical practice for treating patients with breast cancer [1] or melanoma [2]. SLNB is used to assess the tumoral involvement of lymph nodes not only for staging (parameter N of the TNM [tumor, node, metastases] system) and prognostic stratification, but also for therapeutic purposes [3]. This procedure is part of the so-called "radioguided surgery," a whole spectrum of nuclear medicine applications based on the combination of preoperative imaging, intraoperative detection, and postoperative techniques, involving close collaboration between at least three different specialties (nuclear medicine, surgery, pathology, and sometimes radiology and health physics as well) [4].

Originally introduced in the early 1990s, the sentinel lymph node (SLN) procedure optimizes the detection of occult lymph node metastases in patients without clinical evidence of local–regional involvement. The histopathology of the sentinel nodes(s) identified by the procedure, and resected, can distinguish macrometastases (>2 mm in size), micrometastases (between 0.2 mm and 2 mm), and submicrometastases (<0.2 mm), as specified in the 7th edition of the American Joint Committee on Cancer (AJCC) cancer staging manual [5]. This is possible because the pathologist is now able to focus on much fewer lymph nodes than those normally retrieved during conventional radical lymphadenectomy of a certain basin, so a more detailed histopathologic examination of the sentinel node(s) can be carried out, using more histologic sections (to encompass virtually the entire lymph node) and more sensitive techniques (immunohistochemistry in addition to hematoxylin and eosin staining, and even molecular analysis) [5].

Radioguided surgical procedures are generally less invasive and/or less aggressive than traditional surgical approaches. In the case of radioguided biopsy of the SLN, instead of a total lymphadenectomy (for example of the homolateral axilla in breast cancer), patients undergo surgical removal of only one (or a few) lymph node(s), thus reducing both immediate and long-term postsurgical complications, such as lymphedema, motor/sensory nerve damage, and functional impairment of the shoulder/arm. This novel surgical strategy is based on the hypothesis that lymphatic drainage to a regional lymph node basin follows an orderly, predictable pattern, and on the function of lymph nodes on a direct drainage pathway as effective filters for tumor cells. Consequently, all lymph nodes with direct drainage from the primary tumor are considered as sentinel nodes.

At present, SNLB is routinely performed in patients with breast cancer or melanoma, but this application is continuously expanding to other epithelial solid cancers. In fact, the presence or absence of metastasis in the SLN(s) has a significant impact on the therapeutic strategy for breast cancers and melanomas. In patients with early cancer, if the SLN does not contain metastasis, the surgical approach should aim to remove the primary tumor and avoid unnecessary regional node dissection. In fact, it is extremely unlikely that nonsentinel lymph nodes contain metastasis when the sentinel node is free from tumor cells; thus, extensive lymph node dissection is unnecessary in this circumstance. On the other hand, patients whose SLN contains metastasis usually require dissection of regional lymph nodes [6].

Imaging is made possible by interstitial administration at the tumor site of radiolabeled colloid particles that drain from the injection site through the lymphatic system, then selectively accumulate by phagocytosis into the macrophages of the SLNs, with consequent prolonged retention. Colloid

F. Orsini (✉)
Regional Center of Nuclear Medicine,
University of Pisa Medical School, Pisa, Italy
e-mail: federicaors@gmail.com

G. Mariani et al. (eds.), *Atlas of Lymphoscintigraphy and Sentinel Node Mapping*,
DOI 10.1007/978-88-470-2766-4_7 © Springer-Verlag Italia 2013

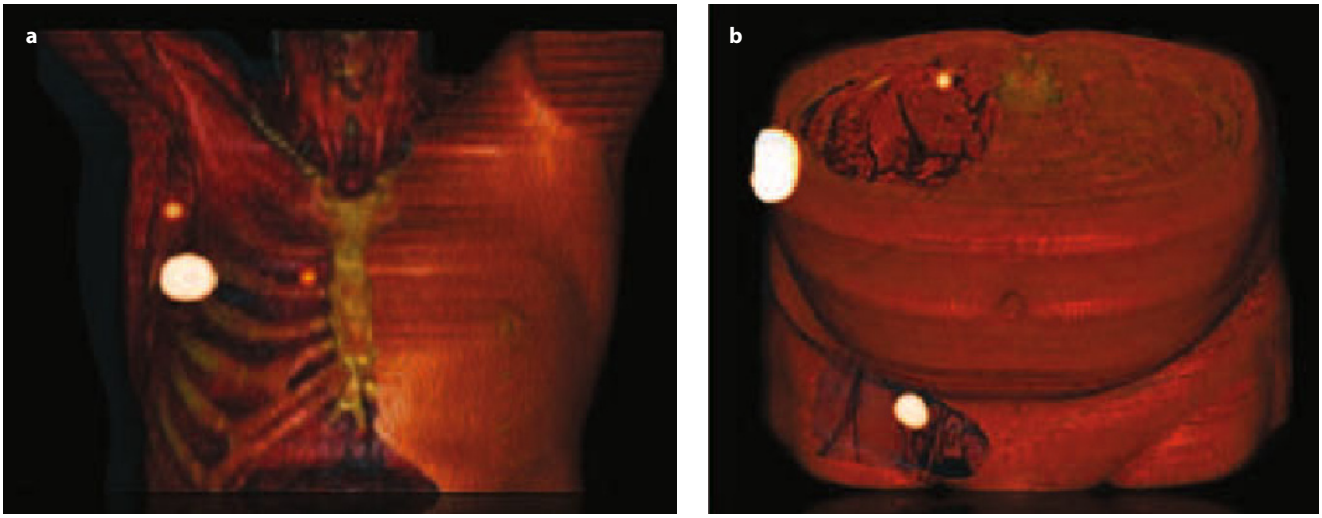

Fig. 7.1 Example of post-processing elaboration of SPECT/CT images. In both cases layers of the tegument have been focally "removed/canceled" asymmetrically between the two sides of the body so to show the underlying anatomy. **a** Lymphoscintigraphy for SLN mapping in a patient with breast cancer, clearly showing migration of ^{99m}Tc nanocolloid both to an axillary SLN and to an internal mammary chain sentinel node. **b** Lymphoscintigraphy for SLN mapping in a patient with melanoma at the right flank, clearly showing migration of ^{99m}Tc nanocolloid both to a sentinel lymph node in the right groin and to a sentinel node in the retroperitoneal area of the abdomen

particles labelled with technetium-99m (^{99m}Tc) are currently used for this purpose. The general term "colloid" indicates a class of macromolecules of micellar size varying in size between about 5 nm and 1000 nm (0.005–1 μm), with similar physicochemical and biological patterns. The speed of lymphatic drainage from the site of interstitial injection, and the amount retained in the SLN, depend mainly on the size of the radiocolloid used, which may be either an inorganic substance (gold-198 [^{198}Au] colloid, ^{99m}Tc–antimony sulfur, ^{99m}Tc–sulfur colloid, ^{99m}Tc–stannous fluoride, ^{99m}Tc–rhenium sulfur), or derived from biological substances (nano- or microcolloidal human serum albumin). Small-sized radiocolloids (smaller than about 100 nm) migrate quite quickly from the injection site through the lymphatic system, but they are not efficiently retained in the sentinel node. On the other hand, larger-sized radiocolloids are retained more efficiently in the SLN, but their migration from the interstitial administration site is slower.

^{99m}Tc–albumin-nanocolloid (which has a quite narrow range of particle size, with over 90% of the particles being smaller than 80 nm) is commercially available and most widely employed in Europe, while ^{99m}Tc-sulfur colloid (with a wide range of particle size between about 20 nm and 400 nm) is widely employed in the USA [7].

Lymphoscintigraphy, a mandatory preoperative step of the entire SLNB procedure, is normally performed with conventional gamma cameras. When the gamma camera is combined with a computed tomography (CT) component to constitute a hybrid SPECT/CT tomograph, the fused images obtained are highly useful, especially in the case of complex anatomical regions and/or unusual lymphatic drainage patterns (Fig. 7.1). In fact, they provide the surgeon with a morphologic and functional roadmap (CT component and SPECT component, respectively) for planning the procedure with minimal surgical access and operating time. For immediate decision-making during surgery, intraoperative exploration of the surgical field is performed with the widely validated procedure based on the so-called hand-held "gamma probe." While this instrumentation produces a numerical readout and an acoustic signal that is proportional to radioactivity accumulation, as a guide in the surgical field, the recently developed portable gamma cameras enable real-time scintigraphic imaging of the surgical field. All these instruments allow selective identification of the SLN(s) to be removed by the surgeon and analyzed by the pathologist. This interaction between technologies and medical disciplines permits continuous refinement of the methodology and improves the outcome of radioguided surgical procedures.

7.2 Preoperative Imaging

Lymphoscintigraphy is generally performed in the afternoon of the day preceding surgery if the operation is scheduled in the early morning, or on the same day 4–6 hours prior to surgery, depending on the logistics of the institution. For same-day procedures, a smaller activity of radiocolloid is generally administered (at least 15–20 MBq) compared to the two-day procedure (at least 37–74 MBq).

The gamma camera energy selection peak is centered on the 140 keV of ^{99m}Tc (with a window of ±10%), and the use of high-resolution collimator(s) and of a 256 × 256 acquisi-

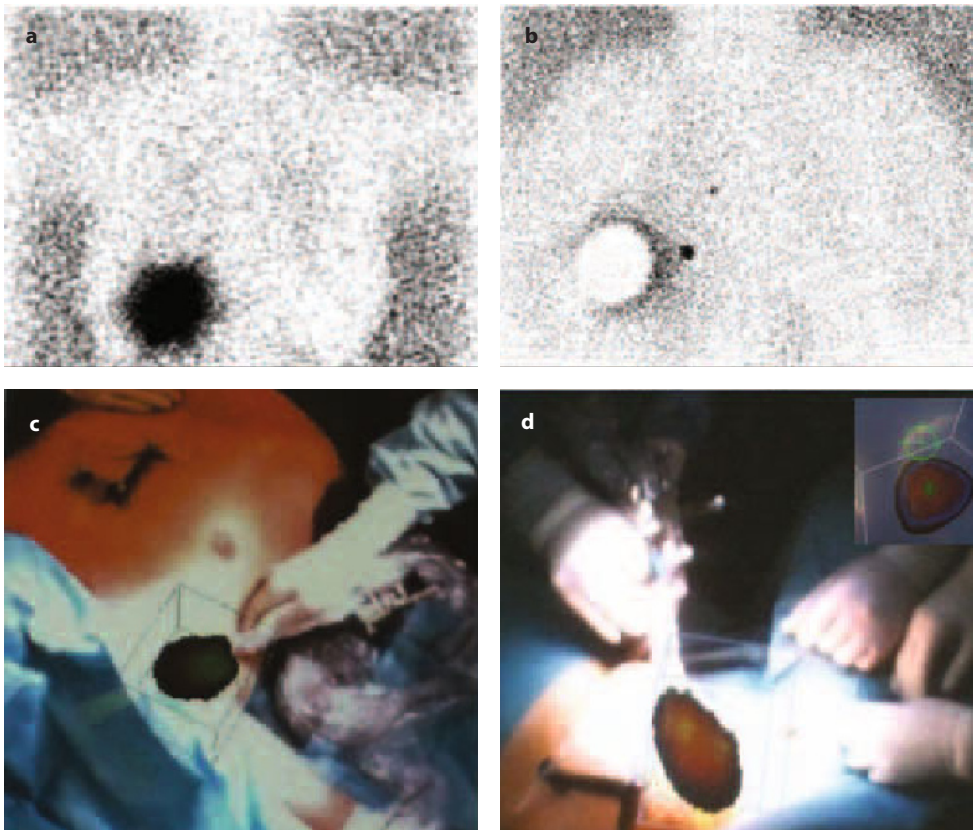

Fig. 7.2 *Upper panels* show planar scintigraphy (with flood phantom for body contour, see further below) obtained in a breast cancer patient about 2 hours after injecting ^{99m}Tc-nanocolloidal albumin intratumorally (**a**). Besides intense radioactivity remaining at the injection site, this image shows no migration of the radiocolloid to axillary SLNs. The *right image* (**b**) was taken 16 hours later, using a lead plate to cover the injection site. A hot spot is depicted in the close vicinity of injection, corresponding to an internal mammary chain SLN. The *lower panels* show overlay of the freehand SPECT 3D image on the intraoperative video image of the same patient, for easier anatomical correlation. **c** Scanning of the axilla without visualization of the lymph nodes. **d** Intraoperative visualization of the sentinel node in the right internal mammary chain (insert in the *upper right square*)

tion matrix is preferred; a pinhole collimator may occasionally be used to improve spatial resolution.

While dynamic acquisition is needed especially when rapid lymphatic drainage is anticipated (melanoma, head and neck, penile, testicular, and vulvar cancer), it can nevertheless also provide relevant information for identifying the actual SLN(s) (versus higher-echelon nodes) in other malignancies, particularly breast cancer. Concerning breast cancer in particular, the patient is positioned supine with her arms raised above the head, and the collimator is placed as close as possible to the axillary region. Anterior, anterior-oblique, and lateral images are acquired. A cobalt-57 (^{57}Co) flood source can be positioned between the patient's body and the collimator, in order to obtain some reference anatomic landmarks in the scintigraphic image (Figs. 7.2 and 7.3). Alternatively, the body contour can be identified by moving a ^{57}Co point source along the patient's body during scintigraphic acquisition (Fig. 7.4).

Besides identifying the SLNs, lymphoscintigraphy is also useful to identify an unusual lymph draining basin, as well as an internal mammary chain or even intramammary, interpectoral, or infraclavicular lymph nodes [8] (Fig. 7.5), or additional sentinel nodes in areas of deep lymphatic drainage such as the pelvis, abdomen or mediastinum. SPECT/CT imaging could be particularly important in these cases. The use of SPECT/CT acquisitions can be directly oriented to the anatomical localization of sentinel nodes, thus obviating the problem of identifying anatomic landmarks as a reference for topographic location of the SLN(s) [9–11].

An additional useful application of SPECT/CT is in cases where the SLN is not visualized on planar imaging. In this situation, only SPECT/CT imaging can allow sentinel node identification; in fact, due to the correction for tissue attenuation, SPECT/CT is usually more sensitive than planar images and may particularly be useful in obese patients (Fig. 7.6). Moreover, SPECT/CT may be necessary for the localization of sentinel nodes in areas with complex anatomy and a high number of lymph nodes (such as the head and neck).

However, SPECT/CT does not replace planar lymphoscintigraphy, but should rather be considered as a complementary imaging modality. In fact, contrary to SPECT/CT, planar lymphoscintigraphy allows the cutaneous projection of the SLN to be marked with a dermographic pen, in order to help the surgeon localize the site for the best surgical access. In current protocols, SPECT/CT is performed following delayed planar imaging (mostly 2–4 hours after radiocolloid administration). This sequence of acquisitions is helpful to clarify the role of both modalities. Planar dynamic acquisitions allow better visualization of the routes of lymphatic drainage. Dynamic acquisition usually consists of sets of a few minutes each (generally 1–5 minutes) or sequen-

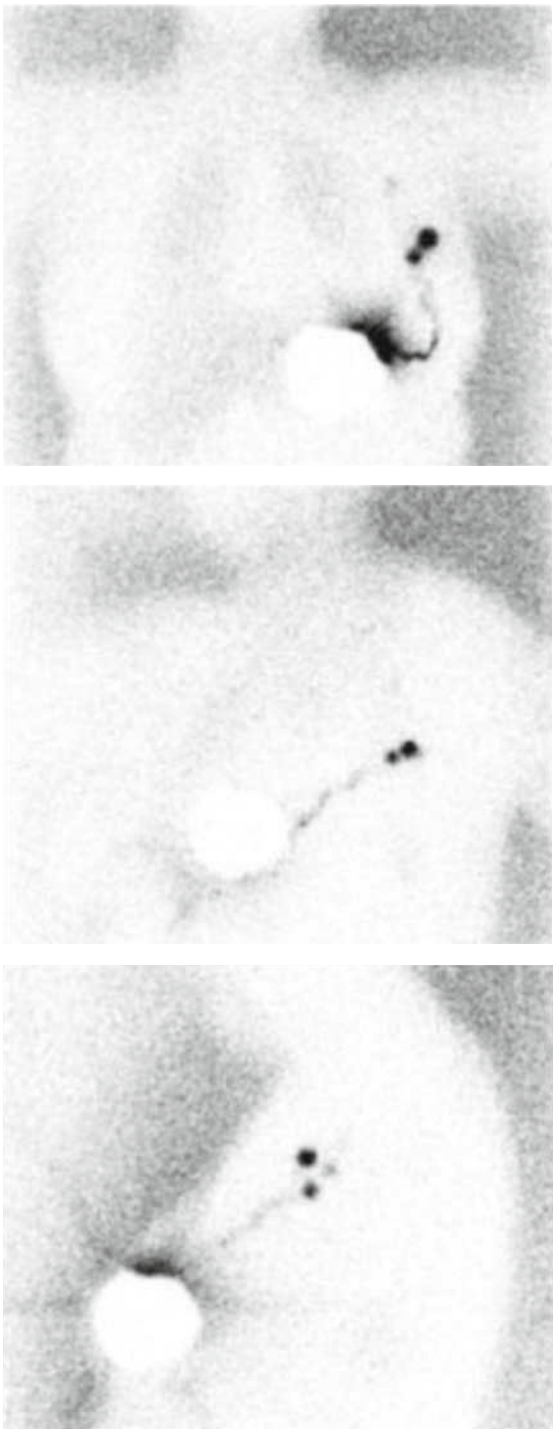

Fig. 7.3 Planar lymphoscintigraphy of a patient with breast cancer obtained between 20 minutes and 30 minutes after injecting about 111 MBq of ^{99m}Tc-nanocolloidal albumin peri-areolarly in a patient with cancer of the left breast. The *upper image* shows an anterior projection, the *central image* an oblique view and the *lower image* a lateral projection. Images were taken using a lead circle to cover the injection site. All images were acquired using a single-head gamma camera and a high-resolution, low-energy collimator (acquisition time 2 minutes). The ^{99m}Tc flood phantom placed opposite the gamma camera head produces the body contour delineation. While two axillary SLNs are visualized in the anterior and oblique projection, three nodes are visualized in the lateral projection

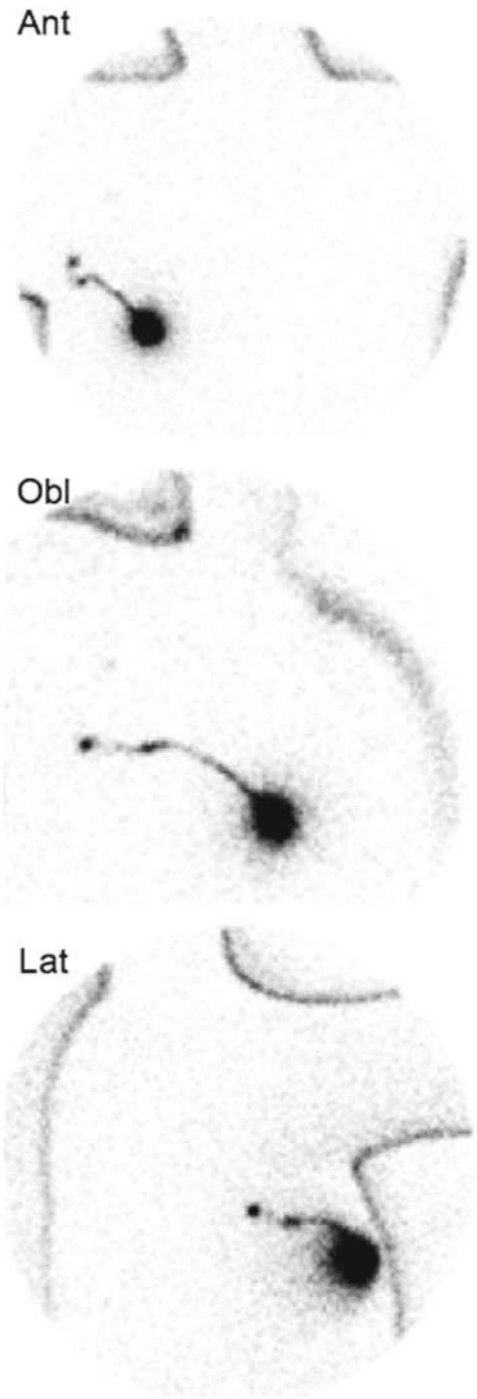

Fig. 7.4 Body contour delineation obtained by moving a ^{57}Co point source along body of the patient during acquisition of the planar scintigraphic images. In this patient with cancer of the right breast, ^{99m}Tc-nanocolloidal albumin was injected peri-areolarly. Images acquired in the anterior projection (*Ant*, upper panel), right anterior oblique projection (*Obl*, central panel), and right lateral view (*Lat*, lower panel) visualize migration of the radiocolloid through a lymphatic channel to a single SLN in the axilla

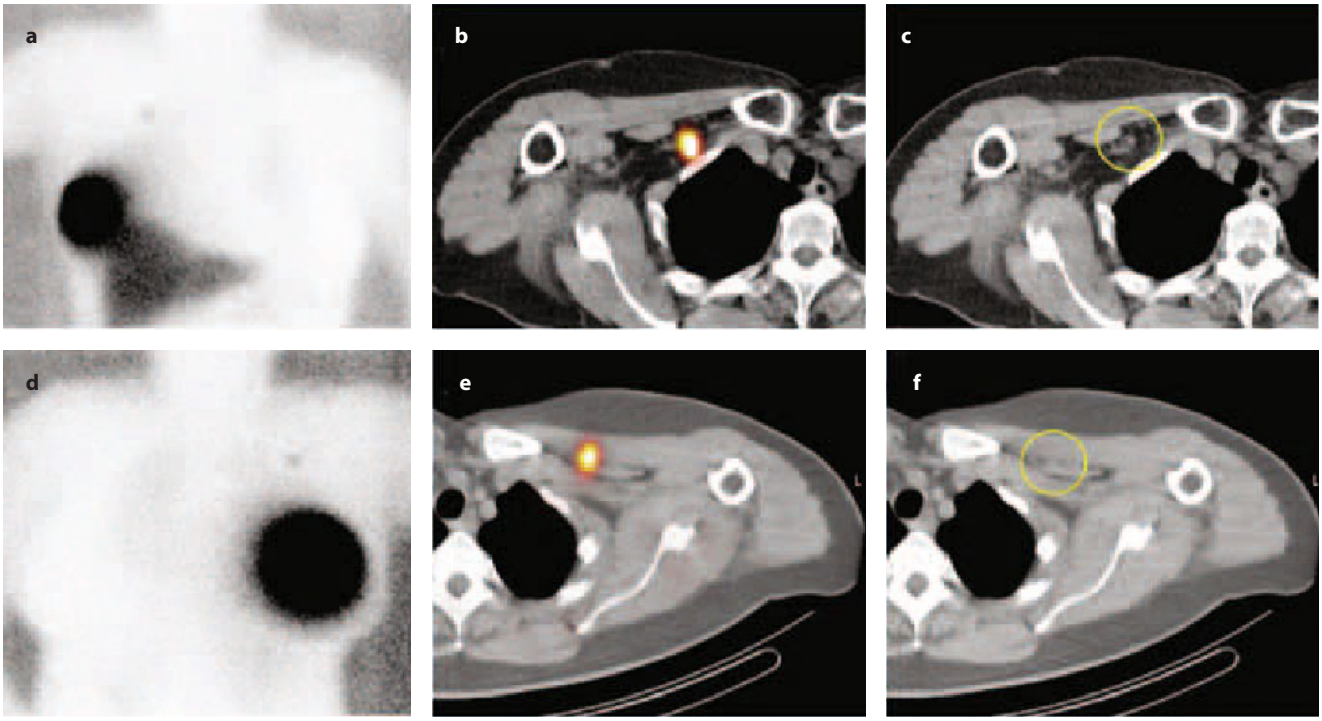

Fig. 7.5 Added value of SPECT/CT imaging in two different patients in whom planar scintigraphy shows focal uptake in the retroclavicular area; the patients had cancer located in the right breast (**a**) and in the left breast (**d**), respectively. **b**, **e** Fused axial SPECT/CT sections, showing the location of the two SLNs between the pectoral muscles. These sentinel nodes correspond to two single lymph nodes in the CT images (**c**, **f**, *yellow circle*), respectively

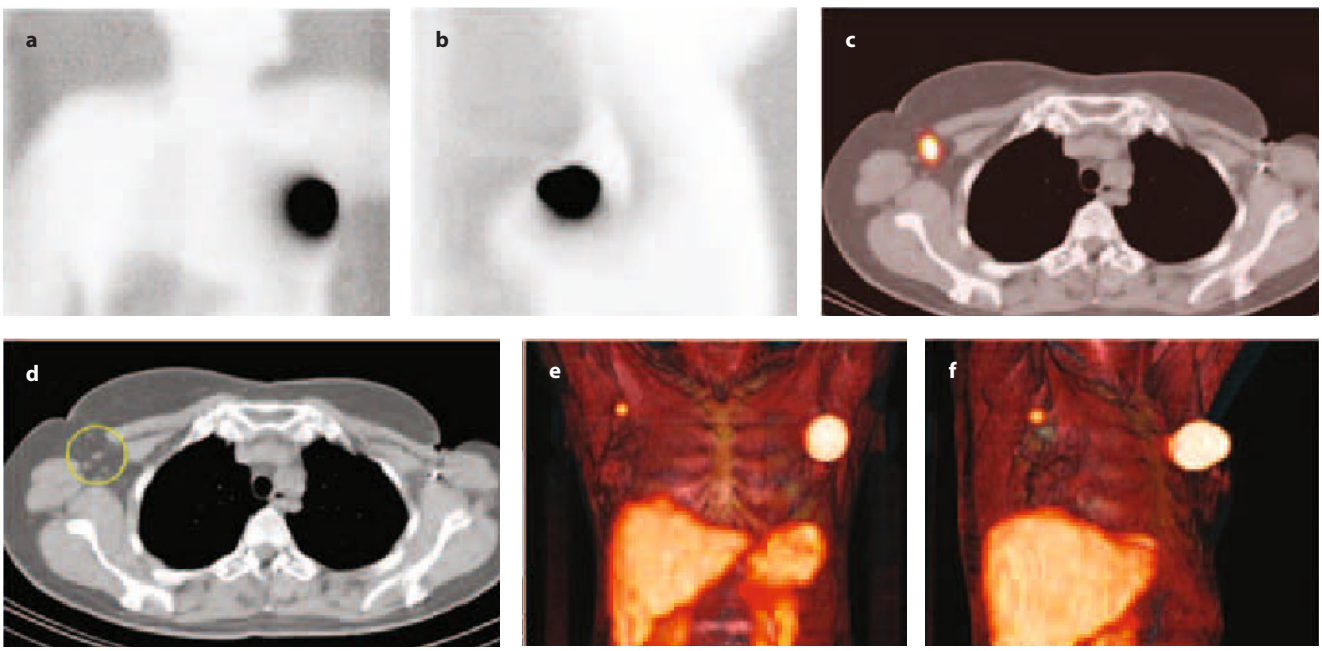

Fig. 7.6 Example of lymphatic drainage to the contralateral axilla in a patient with breast cancer. Anterior (**a**) and left lateral (**b**) planar images show no drainage from the site of intratumoral radiocolloid injection in the left breast (body contour obtained with a flood source placed beneath the patient's body). By contrast, on the fused axial SPECT/CT image, a SLN is clearly visualized at the border of the right pectoral muscle (**c**), corresponding to a single lymph node on the CT image (**d**, *yellow circle*). This SLN is displayed using 3D volume rendering for a better anatomical recognition in the anterior (**e**) and right anterior-oblique views (**f**)

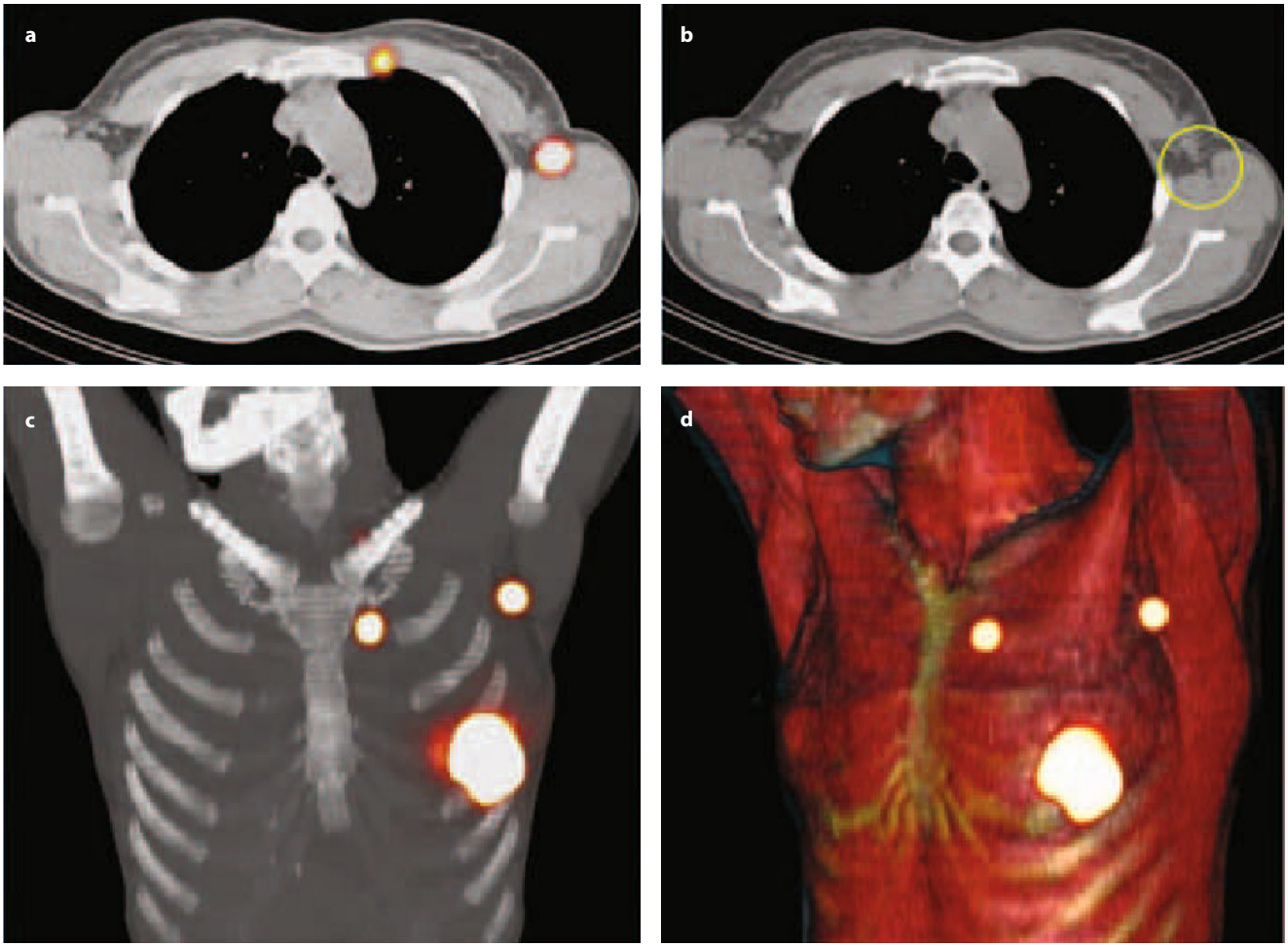

Fig. 7.7 Patient with breast cancer. **a** Fused axial SPECT/CT section obtained during lymphoscintigraphy, showing two SLNs, respectively in the left internal mammary chain and in the left axilla. **b** The *yellow circle* corresponds to a small lymph node seen on axial CT. **c** Fused coronal SPECT/CT displayed as a maximum intensity projection, showing a SLN in the left axilla and an internal mammary chain sentinel node in the second left intercostal space. **d** SPECT/CT with volume rendering for 3D display, showing the two SLNs, respectively in the left internal mammary chain and in the left axilla, with their anatomic localizations with reference to muscles and bones

tial sets of static images in the preset count mode (generally 300,000–500,000 counts) acquired starting immediately after radiocolloid injection until there is clear scintigraphic visualization of the lymphatic routes and SLN(s).

Multiplanar reconstruction (MPR) enables two-dimensional display of fusion images in relation to CT and SPECT, with the use of cross-reference lines allowing navigation between axial, coronal, and sagittal views. At the same time, this tool enables correlation of the radioactive sentinel nodes seen on fused SPECT/CT with the lymph nodes seen on CT (Fig. 7.7a, b). This information may be helpful during the intraoperative procedure, as well as for assessing the completeness of excision using portable gamma cameras or probes.

Fused SPECT/CT images may also be displayed using maximum intensity projection (MIP). This tool enables three-dimensional (3D) display, and improves anatomical localization of SLNs by adding various slices (Fig. 7.7c).

When using volume rendering for 3D display, different colors are assigned to anatomical structures such as muscle, bone, and skin. This facilitates better identification of anatomical reference points and incorporates an additional dimension in the recognition of SLNs (Fig. 7.7d).

7.3 Intraoperative Gamma-probe Guidance

The so-called gamma probe is used to count radioactivity in the surgical field intraoperatively, without producing any

scintigraphic image but yielding both a numerical readout and an audible signal that is proportional to the counting rate.

The detector is usually of limited size, basically a long narrow cylinder with a diameter of 12–18 mm, sometimes slightly angled in order to allow easier handling within the surgical field. The gamma probe can be utilized in the surgical field because it is made of a material that can be sterilized (usually metal), or it can simply be covered with a sterilized wrapping (such as those used for intraoperative ultrasound probes). Through the digital readout and acoustic signal, the gamma probe enables the surgeon to precisely localize areas of maximum radioactivity accumulation, thus guiding identification and removal of the target tissue [12–15].

The commercially available gamma probes can be divided into crystal scintillation and semiconductor probes. Further technical features of the probe vary, depending upon whether the radiopharmaceuticals are labeled with ^{99m}Tc or other radionuclides, including positron-emitting radiopharmaceuticals [16–18].

The probe is connected to a small control unit, equipped with a portable laptop or tablet, usually with a flexible cable that may also be covered with sterilized wrapping; nevertheless, bluetooth-like connections have now become available, permitting easy use of the entire instrument in the operating room. The energy window for detection/counting is usually around 140 Kev (for ^{99m}Tc-labeled radiopharmaceuticals), but can vary depending on the radionuclide employed. At the same time, the unit usually emits an audible signal, the pitch/tone of which varies proportionally to the counting rates. The acoustic signal helps the surgeon to explore the surgical field without looking at the control unit display.

The sensitivity (counting rate per unit of radioactivity), energy resolution (ability to detect "true" counts arising in the target versus secondary scattered radiation), spatial resolution (ability to identify very close radioactive sources as distinct from each other), and linearity of counting (relates to the dead time) are the most important parameters of the probe in detecting radiation. Therefore, the main important tasks of a probe include sufficient sensitivity (to identify a weakly active sentinel node when attenuated by, typically, up to 5 cm of soft tissue) and energy and spatial resolution (to discriminate the activity of a certain energy within the SLN from that originating from other sites).

More recently, with the development of positron emission tomography (PET) techniques, intraoperative probes specifically designed to detect the high-energy gamma rays originating from the annihilation process have become commercially available, thus enabling radioguidance for PET radiopharmaceuticals [19, 20].

Nevertheless, major advances in the whole process of SLN mapping, in both the preoperative and the intraoperative phases, have been made possible by the use of SPECT/CT and/or intraoperative imaging probes. In fact, hybrid imaging with SPECT/CT supplies the surgeon with anatomotopographic information that guides resection through the optimal surgical access according to the principle of least invasive surgery [21, 22].

As exemplified in Fig. 7.8, this approach is especially useful when planning surgery in complex anatomical regions such as the head and neck or the pelvis [23–29].

Just before starting surgery, and with the patient already positioned on the operating table, the gamma probe is initially utilized to scan the sentinel lymph nodal basin(s) and/or any other region where radiocolloid accumulation has been visualized, in order to confirm correct identification of the SLN(s). Using the images and skin markings as guides, the probe (placed over the regions of highest counts) can be used to select the optimum location for incision. After incision, the probe is then introduced through the surgical field to explore the expected localization of the sentinel nodes, which are usually easily identified by acoustic signal on the basis of high target/background count rates. After removing the lymph nodes, the operative field is explored again with the probe, assessing residual radioactivity to confirm removal of the hot node(s). If necessary, the search must continue for possible further radioactive lymph nodes. The SLN and any other nodes so identified are then sent for complete histopathologic analysis.

Counts are recorded per unit time with the probe in the operative field, over the node, before excision (in vivo) and after excision (ex vivo). A background tissue count is also recorded with the probe pointing away from the injection site, nodal activity, or other physiologic accumulations (i.e., liver) [30].

In breast cancer, once the learning phase of SLNB has been completed, the success rate of lymphoscintigraphy and intraoperative gamma-probe counting in identifying SLN(s) is higher than 96–97% in experienced centers. This value is greater than that commonly experienced using blue dye alone (75–80%), while combining radioguidance with the blue dye leads to a 98–99% success rate in SLN identification [31]. Blue dye can be injected around the primary tumor or scar (in a similar way to how the radiocolloid was injected) 10–20 minutes prior to the operation. Administration should be performed after the patient is anaesthetized, to avoid a painful injection. Within 5–15 minutes, the SLN is colored. Currently, the most commonly used dyes are patent blue V, isosulfan blue, and methylene blue. The additional value of dyes may be observed in cases with macrometastasis in the SLN. In fact, such SLN involvement may inhibit radiocolloid accumulation, if tumor cells have replaced most of the normal lymph node tissue [32]. In these cases a new first draining node is seen (Fig. 7.9) [33]. A notable disadvantage of using blue dyes instead of radiotracers is that blue dyes are not helpful if extra-axillary nodes (internal mammary or supraclavicular) are to be evaluated [34, 35].

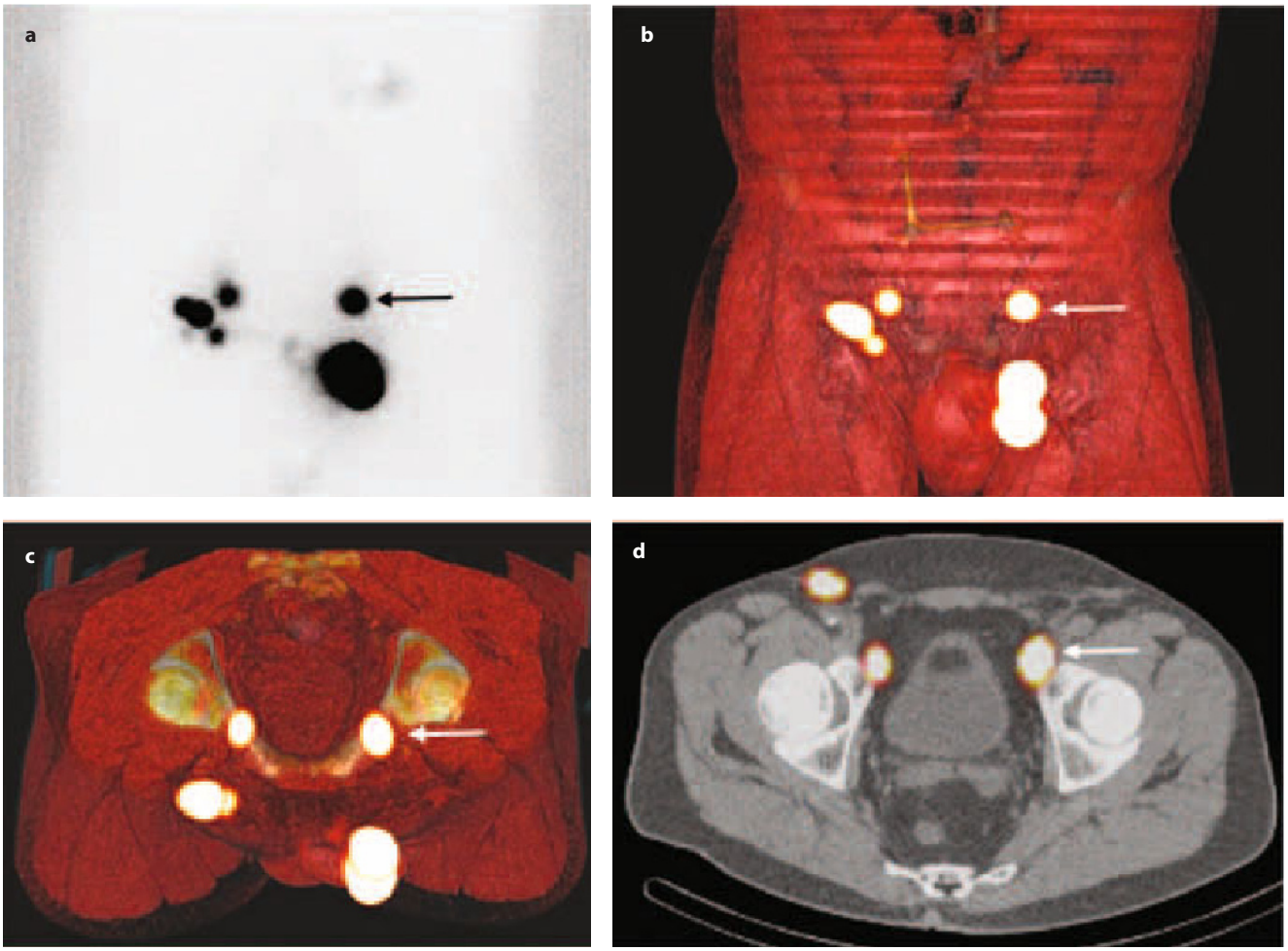

Fig. 7.8 Lymphoscintigraphy in a patient with penile cancer, where the different panels correspond to different modalities of representation and the arrow indicates the same SLN on the left side, correctly assigned to a specific topographic location on the basis of tridimensional imaging. **a** Planar anterior image showing lymphatic drainage to both sides, seemingly to groin lymph nodes (single SLN on the left, *arrow*). **b** SPECT/CT with volume rendering for 3D display in the anterior view (again to seemingly groin SLNs; the *arrow* points to the same SLN indicated in panel **a**). **c** SPECT/CT with volume rendering for 3D display in a cranial view (the bottom side corresponds to the anterior side of the body) showing bilateral external iliac SLNs (the *arrow* indicates the SLN now correctly classified as external iliac SLN). **d** Fused axial SPECT/CT section showing anatomic location of three of the lymph nodes (two on the right and one on the left) at different depths in the pelvis (the *arrow* indicates the left external iliac SLN)

7.4 Intraoperative and Multimodality Imaging

Currently, the trend of surgery is towards adopting minimally invasive approaches for a growing spectrum of procedures. This includes oncological surgery, as it implies much faster post-surgical recovery of patients. For optimally planning and performing these approaches, the most crucial issue is accurate preoperative characterization of the surgical procedure, which is achieved through diagnostic imaging. In this regard, maximum benefit for the success of minimally invasive surgery derives from integration of anatomical (e.g., CT) and metabolic/functional imaging, the latter being typically provided by nuclear medicine procedures. These features contribute to a better characterization of the lesion to be removed, and in many cases enable subsequent intraoperative guidance through the use of devices particularly designed for this use [36, 37].

During the last decade, intraoperative imaging probes have become commercially available for clinical practice, and the use of such hand-held portable gamma cameras is now increasing. By providing real-time imaging with a global overview of all radioactive hot spots in the whole surgical field [38], intraoperative imaging with portable gamma cameras can be used during either open surgery or laparoscopic procedures; the information so gained can be combined with data obtained with conventional or laparoscopic gamma-probe counting [39, 40].

There are several recent reports on the use of portable

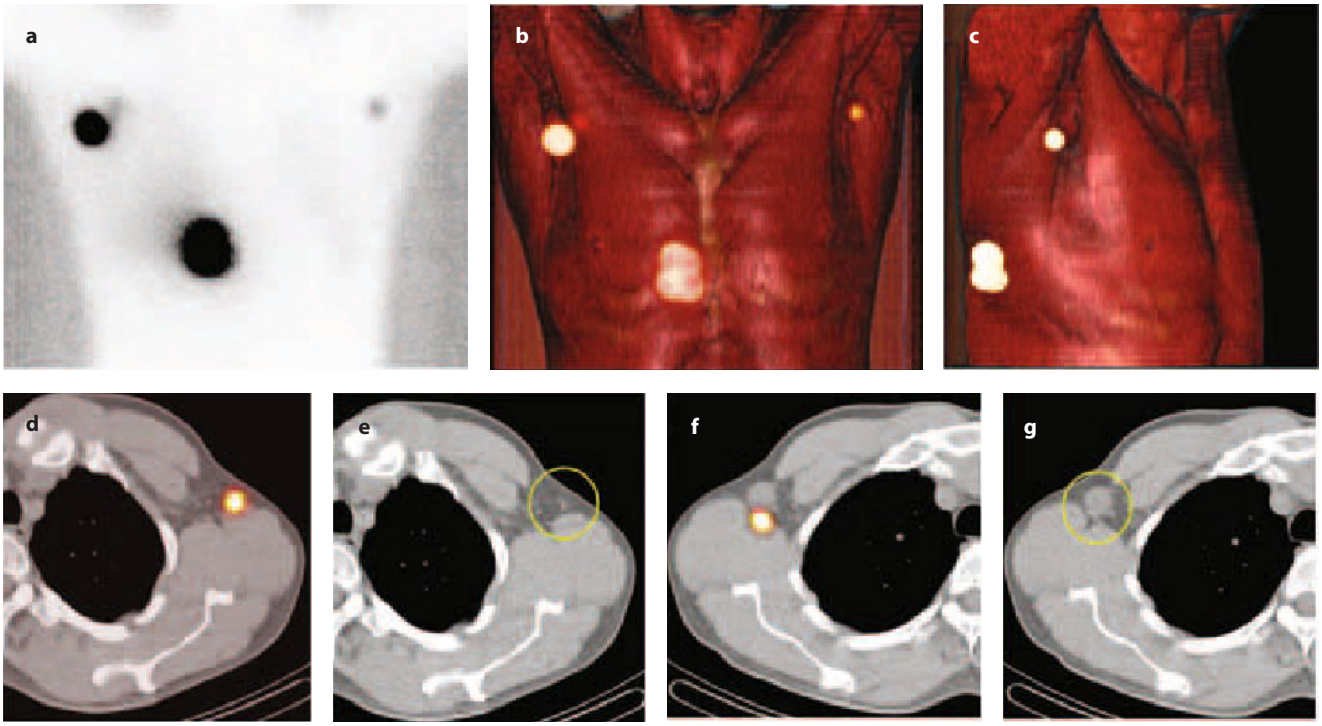

Fig. 7.9 Patient with melanoma located in the back of the right torso. **a** Planar anterior view showing lymphatic drainage to both axillae, as better demonstrated by SPECT/CT with volume rendering for 3D display, respectively in the anterior and in the right oblique view (**b** and **c**). **d–g** Fused axial SPECT/CT section at two different levels, showing the location of radioactive lymph nodes, in the left axilla (**d**) and right axilla (**f**). The corresponding CT sections show that the hot lymph node in the left axilla corresponds to a normal-sized node (*yellow circle* in **e**), while in the right axilla the hot lymph node (of approximately normal size) is located posterior to a grossly enlarged, most likely metastatic, lymph node not visualized by lymphscintigraphy (*yellow circle* in **g**)

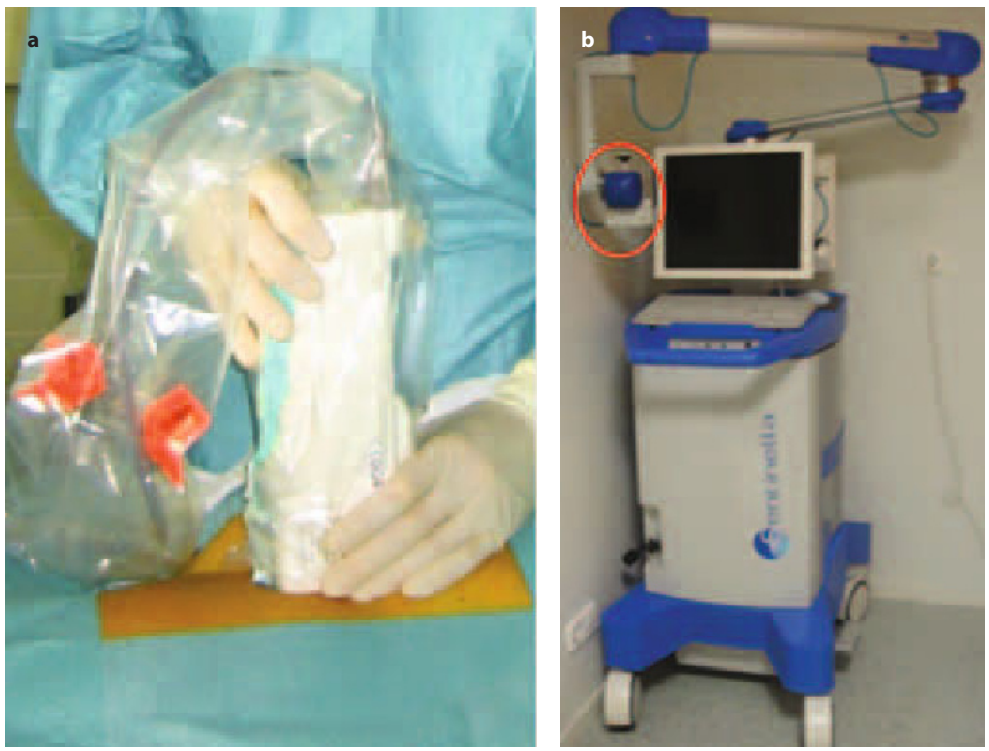

Fig. 7.10 Examples of portable gamma cameras. **a** light-weight portable gamma camera (less than 1 kg), without support system. **b** latest-generation portable gamma camera with improved ergonometry and adequate and stable support system for intraoperative use; this unit incorporates a laser pointer to center the image and adjust the scanning procedure

gamma cameras in clinical and experimental settings. These devices play a remarkable role in the incorporation of imaging during surgery and can be combined with the information obtained preoperatively by lymphoscintigraphy or SPECT/CT. Using the anatomic landmarks of SPECT/CT, the portable device can be oriented to surgical targets in the operating room [41]. There is no delay between image acquisition and display (real-time imaging), with the possibility of continuous monitoring and spatial orientation on the screen. Real-time quantification of the count rates recorded should also be displayed.

The development of such cameras is shown in Fig. 7.10. While the first devices were heavy hand-held devices, the new generation of such equipment includes portable gamma cameras that are lighter, or equipped with stable support systems.

Among the products commercially available, one of the most used devices is equipped with a CsI(Na) (cesium iodide doped with sodium) continuous scintillating crystal and different collimators (pinhole collimators, 2.5 mm and 4 mm in diameter, and divergent). The pinhole collimator can enable visualization of the whole surgical field (depending on the distance between the camera and the source). The field of view varies between 4 × 4 cm at 3 cm from the source and 20 × 20 cm at 15 cm from the source. This device has been integrated in a mobile and an ergonomic support that is easily adjustable. The imaging head is located on one arm that allows optimal positioning on the specific area to be explored.

Another approach is based on the use of cadmium zinc telluride (CdZnTe) as the radiation detector. For instance, the detector is made of a single tile of CdZnTe, patterned in an array of 16 × 16 pixels at a pitch of 2 mm. The head is equipped with a series of interchangeable parallel-hole collimators to achieve different performances in terms of spatial resolution and/or sensitivity. The field of view is 3.2 × 3.2 cm and the weight is 800 g [42].

A further development is represented by an intraoperative gamma camera that is still based on the CdZnTe pixel technology, and has originally been developed for breast imaging. The field of view is 13 × 13 cm and the intrinsic spatial resolution is 2 mm. This camera is also equipped with interchangeable parallel-hole collimators and is integrated in a workstand articulated arm.

However, since nonimaging probes are still the standard equipment for detection of radiolabeled tissue in the operating room, the role of intraoperative imaging is generally limited, at least so far, to constituting an additional aid to the surgeon for identification of the SLN. Some authors have tried to assess the added value of portable gamma cameras in clinical practice. Their usefulness in patients with breast cancer is being established in the following conditions: (a) when no conventional gamma camera is available; (b) in particular cases with difficult drainage or extra-axillary drainage (intrammamary and internal mammary chain nodes) [43]; (c) in cases of only faint lymph nodal radiocolloid uptake; (d) when the SLN is located very close to the injection site; or (e) in cases of significant photon emission and scatter from the injection site. In fact, the position of the portable gamma camera can be changed and adjusted in such a manner as to acquire special-angle views, so that sentinel nodes near the injection area can also be shown.

Moreover, some studies have reported detection of SLNs that had been missed when only the gamma probe was used. In fact, using an intraoperative imaging device implies the possibility of monitoring the lymphatic basin before and after removal of the hot nodes, in order to verify the completeness of lymph node excision [44] (Fig. 7.11). After excision of each lymph node, a new image is acquired and compared with the image acquired before excision (Fig. 7.12). If focal radioactivity remains at the same location, it is concluded that another possible SLN is still in place. Thus, the use of a portable gamma camera in addition to the gamma probe appears valuable in providing certainty about whether the sentinel nodes have been adequately removed (Fig. 7.13). Removing extra nodes that probably receive direct lymph drainage from the tumor should be weighed up against the fact that the surgical time is prolonged. However, even if additional time is needed, this extra time may be sufficiently useful in the context of sentinel node procedures that are likely to be difficult, since the use of the gamma camera might reduce the possibility of missing a malignant sentinel node [45, 46].

Discrimination between the true SLN and a second-tier radioactive node is based on the radioactive counts simultaneously recorded with the portable, small-field-of-view cameras, and can be related to the preoperative scintigraphic images. Although the majority of these cases can be solved with the presurgical information provided by SPECT/CT, real-time images acquired with a portable gamma camera enhance the reliability of using the gamma probe, by adding a clear image of surgical fields [47], and could represent an alternative to hybrid imaging.

In the operating room, the gamma camera can be placed above the previously marked sentinel node locations using some external point sources (such as barium-133 [^{133}Ba], gadolinium-153 [^{153}Gd] or iodine-125 [^{125}I]); alternatively, in some gamma cameras a laser pointer is fitted to the device. In those devices where a laser pointer is included (Sentinella; Oncovision), it is displayed as a red cross over the patient's skin. The position of this red cross is visible on the equipment's computer screen.

During surgery, an initial 30–60-second image is acquired with the gamma camera, to assess the surgical field and validate sentinel node uptake. This time can be longer when the lymph nodes are depicted as areas with faint focal uptake. After incision, if there is any difficulty in finding

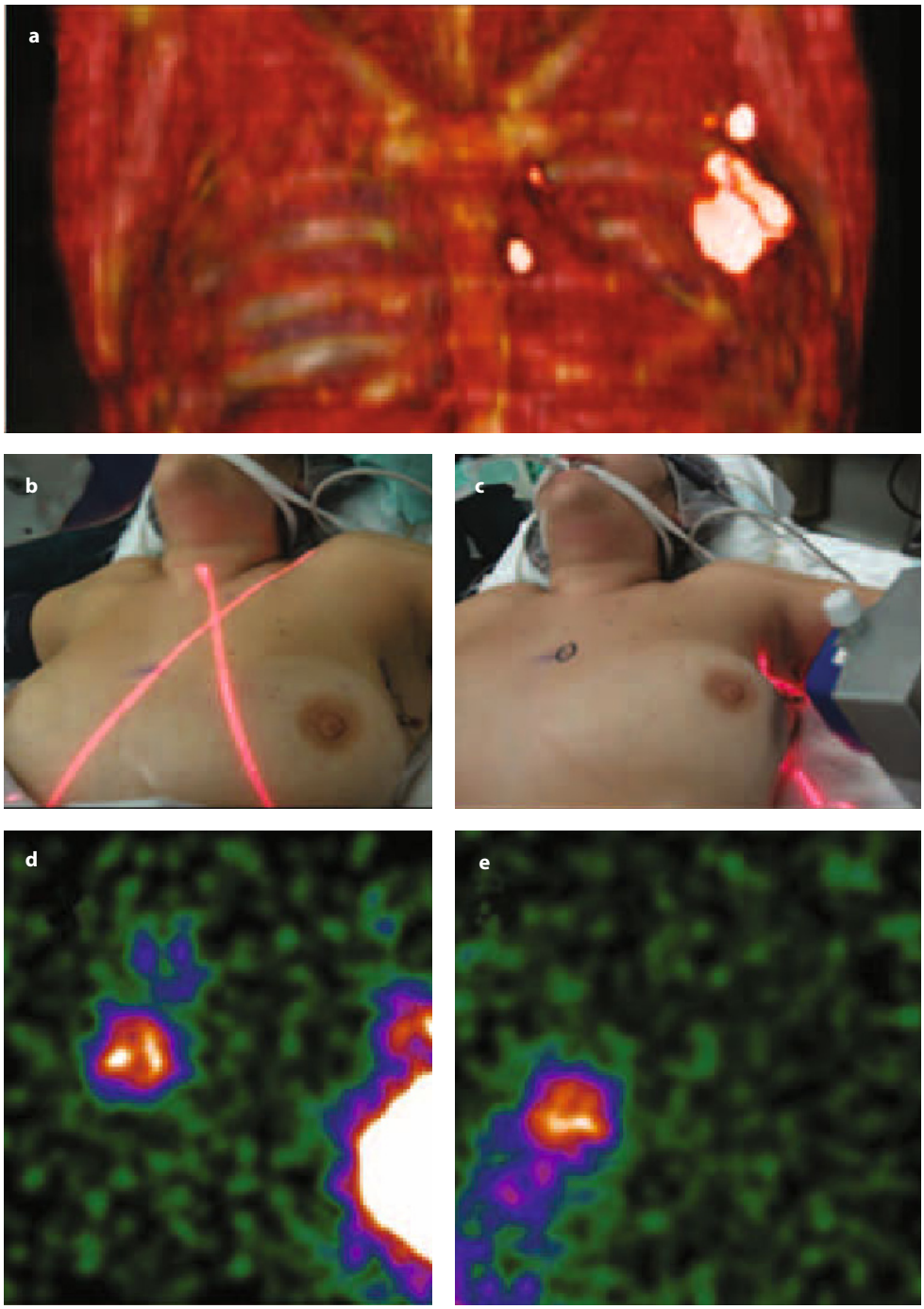

Fig. 7.11 Preoperative images in a 42-year old patient with a T1 cancer in her left breast. **a** 3D reconstruction image after processing SPECT/CT data. **b** A scintigraphic anterior view is acquired by placing the portable gamma camera in previously marked points on the skin (inner mammary chain, see laser cross-pointers). **c** The portable gamma camera can be placed in different positions to better depict the lymph nodes; in this picture it is tilted in an oblique view. **d** Visualization of an inner mammary chain lymph node, with partial vision of the injection site (image corresponding to position of the gamma camera as in **b**). **e** Visualization of an axillary lymph node depicted with the gamma camera positioned as in **c**

the precise location of the sentinel node using the gamma probe, another 30–120-second image, depending on the level of lymph node uptake, is acquired using the portable gamma camera.

The use of the external point sources facilitates SLN localization, as these sources can be depicted separately on the screen of the portable gamma camera, thus functioning as a pointer in the search for the nodes. The matching of two signals (^{99m}Tc signal and ^{153}Gd, ^{133}Ba, or ^{125}I pointer signals) indicates the correct location of the sentinel nodes. This location is then checked using the gamma probe. After sentinel node retrieval, another set of images is acquired to ascertain the absence of the previously visualized sentinel nodes, or to ascertain the presence of remaining nodes (additional sentinel nodes or second-tier nodes [Fig. 7.14]).

Thanks to novel technological possibilities, combining a spatial localization system and two tracking targets to be fixed on a conventional hand-held gamma probe results in

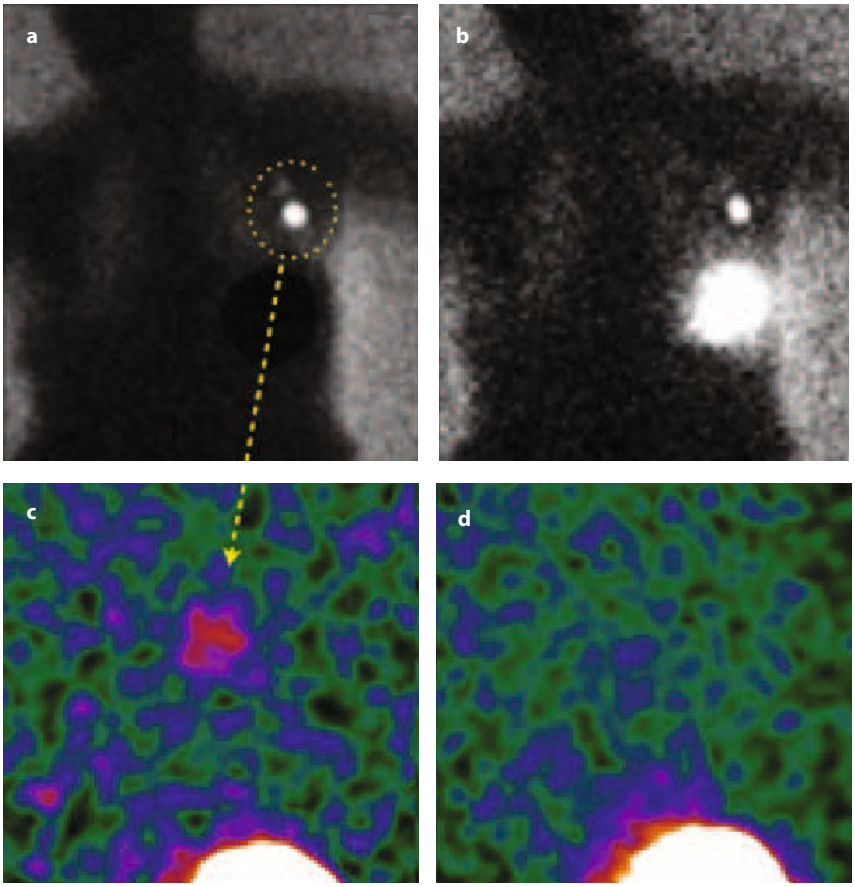

Fig. 7.12 A 57-year-old patient with breast cancer in her left upper outer quadrant. **a** Lymphoscintigraphic image acquired with a conventional, large-field-of-view gamma camera 2 hours after intratumoral injection of 111 MBq of ^{99m}Tc-nanocolloid; at least one axillary SLN is clearly depicted (*yellow circle*). **b** The same image without lead shielding of the injection site shows similar radiocolloid distribution. **c** Operating room image obtained with a portable gamma camera prior to starting the SLN procedure, confirming similar findings (*yellow arrow*). **d** Image obtained with the portable gamma camera after completing radioguided SLN excision, showing no residual activity except in the intratumoral injection site. The use of the portable gamma camera, in addition to the hand-held, nonimaging gamma probe, was especially useful to confirm the completeness of SLN removal

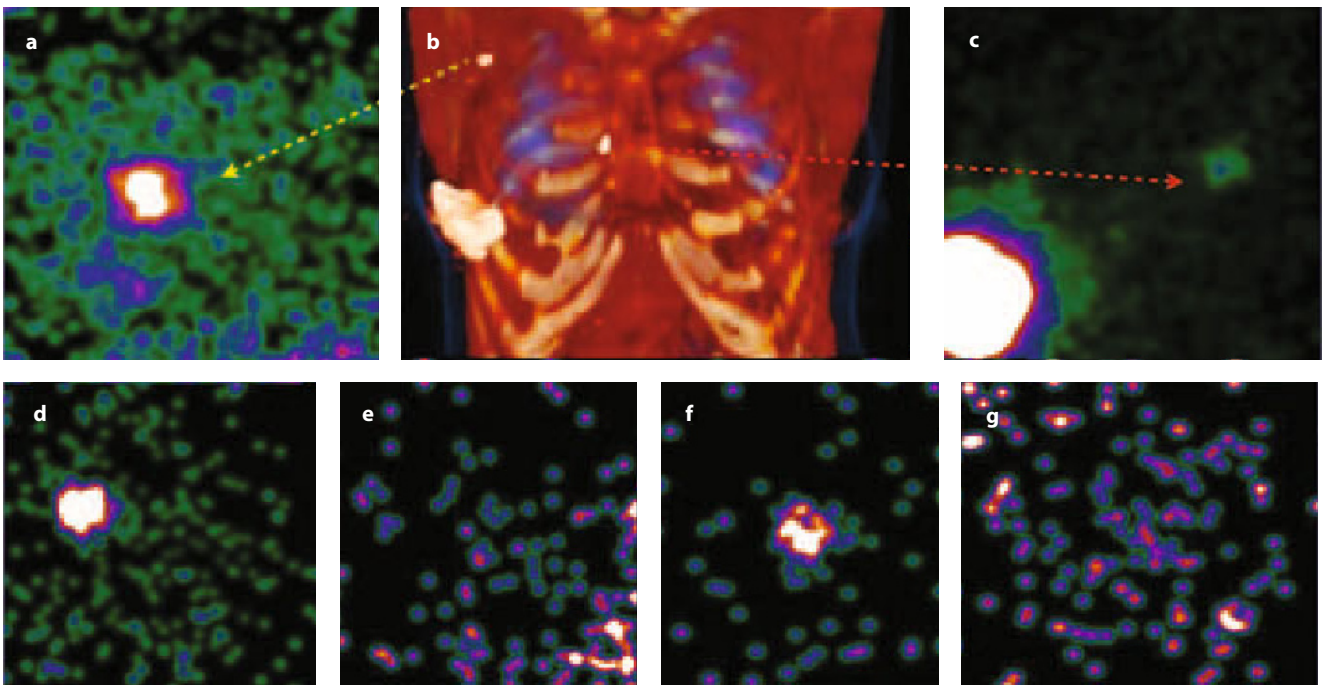

Fig. 7.13 Utility of the portable gamma camera during surgery for the certainty of SLN resection. **a** Radiotracer uptake displayed on gamma camera, corresponding to the node depicted in the axillary area (*yellow arrow*) on the 3D volume rendering reconstruction of a breast cancer patient with lymphatic drainage to the axilla and inner mammary chain (**b**). **c** A parasternal sentinel node (*red arrow*) is also depicted with the gamma camera. **d** Preoperative image of the axilla showing a highly active sentinel node. **e** Image after axillary node retrieval informs about the absence of other significant tracer uptake. **f**, **g** A similar approach in the internal mammary chain sentinel node

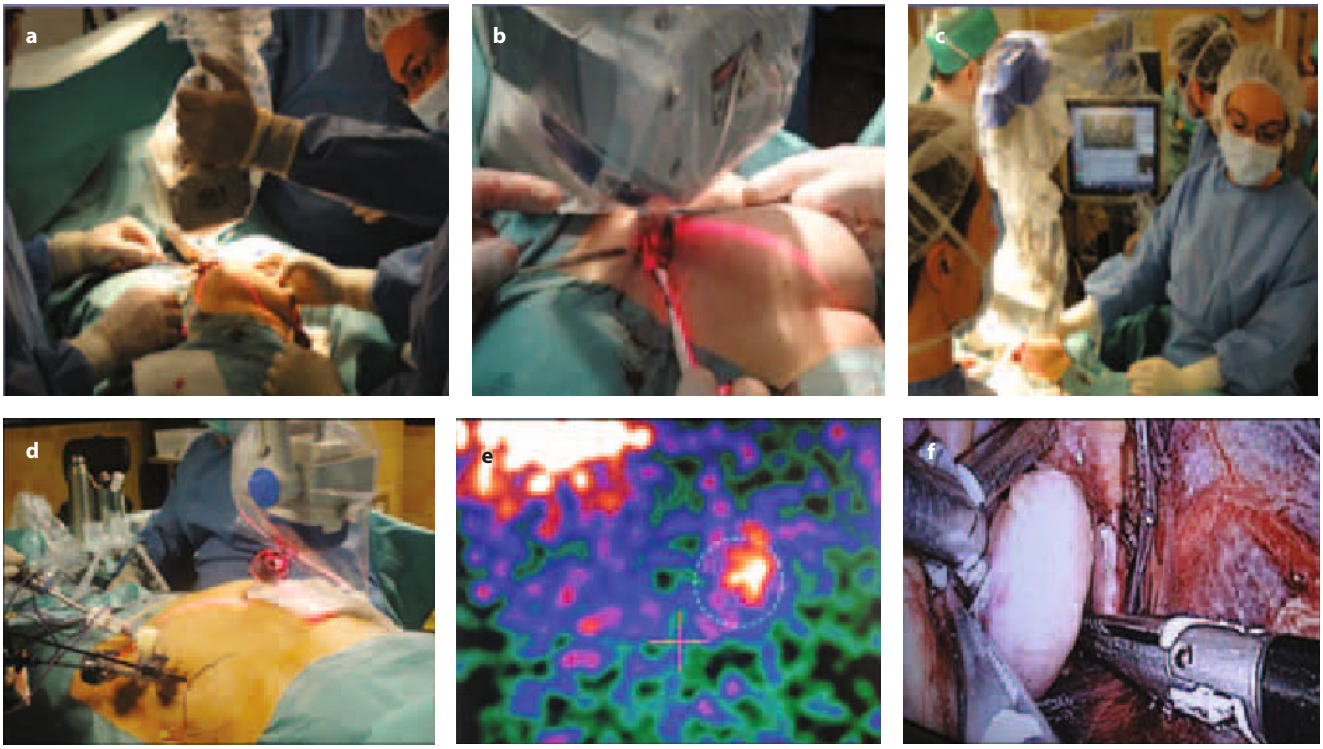

Fig 7.14 Portable gamma camera intraoperative approach. **a** The device is placed over the area of interest in the most convenient way. **b** A red cross shows the central position of image on the gamma camera's screen. **c** This feature allows a better understanding and awareness of the potential sentinel nodes on the surgical field. **d–f** Laparoscopic approach. **d** The portable gamma camera is positioned over abdominal wall to continuously assess the tracer uptake. **e** Usual uptake in a sentinel node close to the common iliac vein (*green circle*). **f** This node was clearly located in that area and subsequently removed

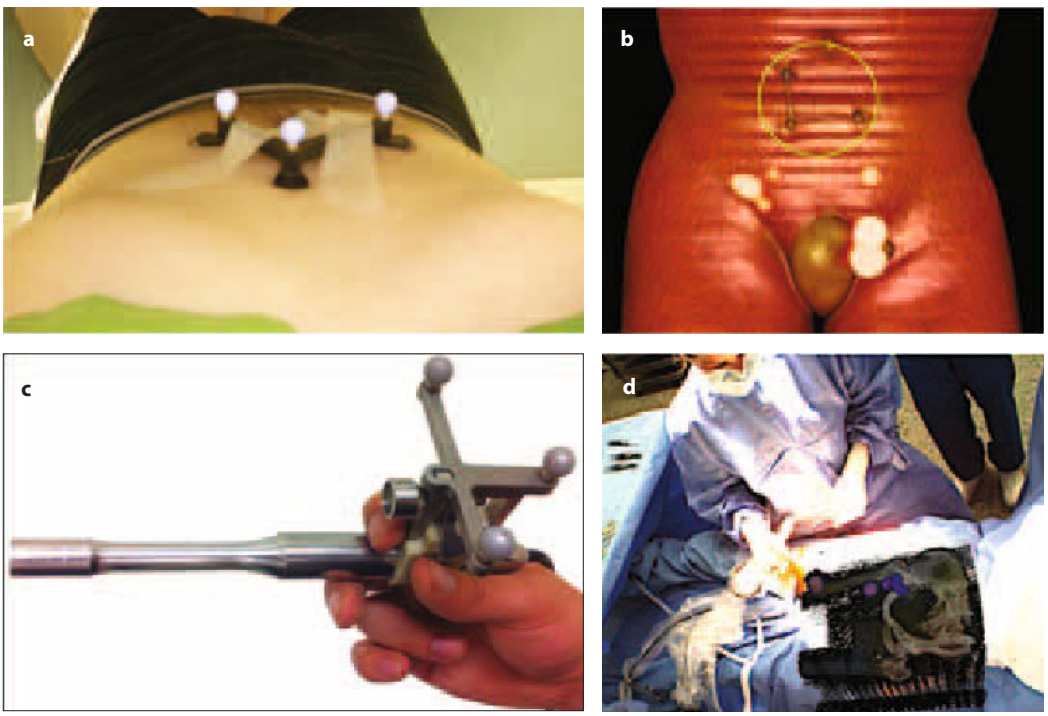

Fig. 7.15 Patient with penile cancer (same patient as in Fig. 7.8). **a** Positioning of the tracking device on the patient's body for radioguided SLNB. **b** 3D volume rendering SPECT/CT, showing the pattern of lymphatic drainage (the approximate position of the tracking device on the patient's body is also indicated in the *yellow circle*). **c** Tracking device attached to a gamma probe in order to generate freehand SPECT data. **d** By integrating preoperative SPECT/CT data, it is possible to overlay the generated 3D image to the patient's body, with simultaneous display of the SLNs on the right side of the pelvis

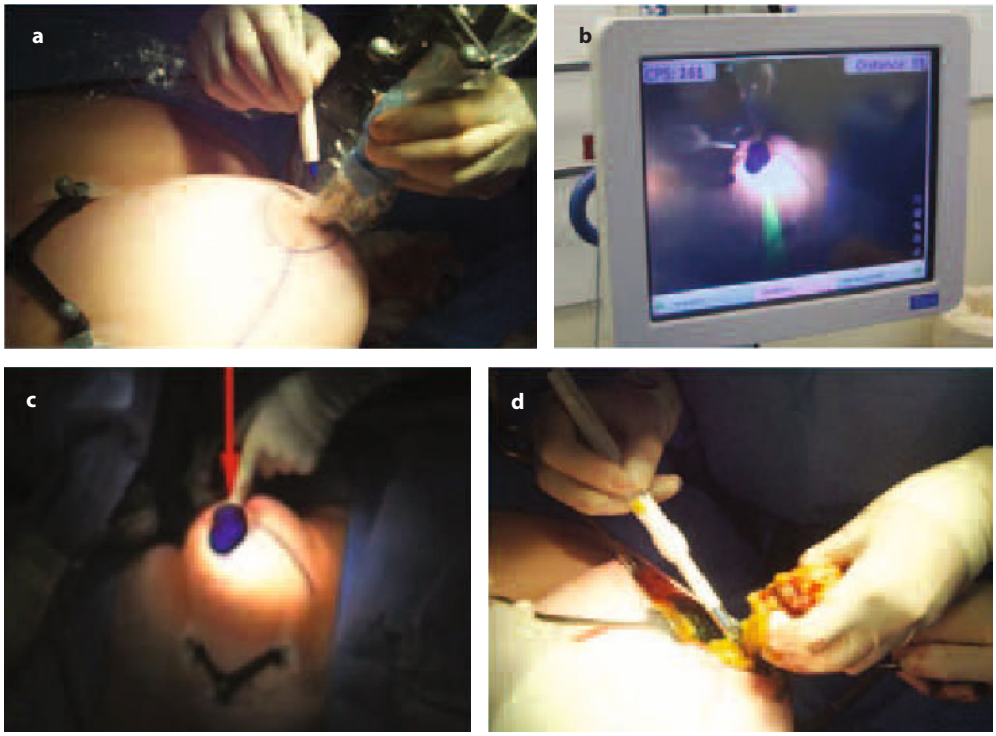

Fig. 7.16 Freehand SPECT-based device system used for radioguided occult lesion localization (ROLL) in a patient with nonpalpable breast cancer. **a** Surgical approach for ROLL; the tracking device positioned on the patient's body is visible on the left. **b**, **c** Overlay of freehand SPECT 3D images on the video displays, with the red arrow in **c** indicating the site of the tumor. **d** Completion of lumpectomy guided by the freehand SPECT-based system

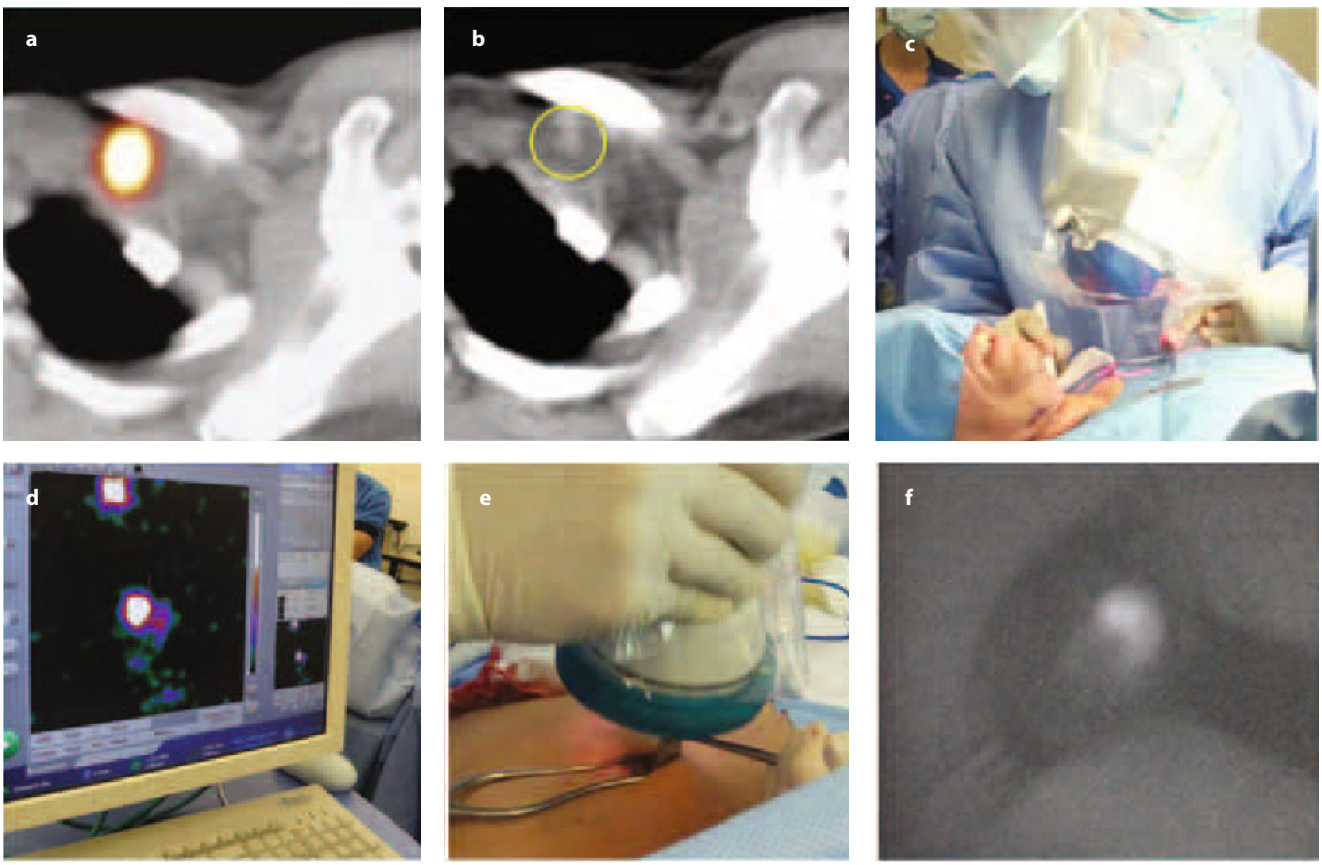

Fig. 7.17 Patient with breast cancer. **a** Fused axial SPECT/CT section showing a radioactive SLN in the left cervical area. **b** This focus of radioactive accumulation corresponds to a solitary lymph node seen in the CT section (*circle*). **c** The use of a portable gamma camera permits the surgeon to select the site for incision, and **d** also to monitor the procedure with intraoperative imaging guidance. The recent introduction of bimodal tracers for simultaneous radioguided (**e**) and fluorescent (**f**) detection is leading to the additional use of a fluorescence camera to better distinguish the SLN in anatomically complex areas

new 3D visualization of the traditional acoustic signal of the gamma probe. This feature, together with the real-time information on depth that the system may provide, expands the application of radioguided sentinel node biopsy in oncology, particularly for malignancies with deep lymphatic drainage [48, 49].

In this regard, the most recent interesting development in radioguided surgery is the system of so-called "freehand SPECT," in which a continuous positioning system installed in the operating room is based on a fixed pointing device, on the patient's body and, correspondingly, on the hand-held gamma counting probe, thus permitting a virtual reconstruction in a 3D environment. The position of the gamma probe relative to the fixed device is tracked by infrared positioning technology, and the output of the intraoperative gamma probe is spatially coregistered in the surgical field (depicted by a video camera) and displayed on a monitor in which the surgeon can easily check the location and depth of the foci of radioactivity accumulation to be resected. This 3D information may be further used for precise localization and targeting of the radioactive SLN(s) and of tumor tissue, thus implementing a radioguided navigation system. The device can ensure permanent assistance and transparent documentation of soft tissue removal during the intervention (Figs. 7.15 and 7.16).

On the other hand, the possibility of combining the current radiopharmaceuticals with other agents opens new fields to explore. In this regard, a radiolabeled nanocolloid agent has been combined with indocyanine green (ICG), a fluorescent agent, for sentinel node detection in robot-assisted lymphadenectomy [50].

In contrast to the use of a single fluorescent agent [51, 52], this bimodal tracer may allow the surgeons to integrate the standard approach based on radioguided detection with a portable gamma camera with a new optical modality based on fluorescent signal detection. This approach is being successfully applied in various malignancies (Fig. 7.17).

For all these new intraoperatives modalities, the preoperative anatomical SPECT/CT acquisition remains essential and is the starting point for surgical planning.

References

1. Kell MR, Burke JP, Barry M, Morrow M (2010) Outcome of axillary staging in early breast cancer: a meta-analysis. Breast Cancer Res Treat 120:441–447
2. Valsecchi ME, Silbermins D, de Rosa N et al (2011) Lymphatic mapping and sentinel lymph node biopsy in patients with melanoma: A meta-analysis. J Clin Oncol 29:1479–1487
3. Giuliano AE, Hunt KK, Ballman KV et al (2011)Axillary dissection vs no axillary dissection in women with invasive breast cancer and sentinel node metastasis: a randomized clinical trial. JAMA 305:569–575
4. Orsini F, Rubello D, Giuliano AE et al (2012) Radioguided surgery. In: Strauss HW, Mariani G, Volterrani D, Larson SM (eds) Nuclear oncology: pathophysiology and clinical applications. Springer, New York (in press)
5. Breast. In: Edge SB, Byrd DR, Compton CC et al (eds) (2010) AJCC Cancer staging manual, 7th ed. Springer, New York, pp 347–376
6. Giuliano AE, Han SH (2011) Local and regional control in breast cancer: role of sentinel node biopsy. Adv Surg 45:101–116
7. Obenaus E, Erba PA, Chinol M et al (2008) Radiopharmaceuticals for radioguided surgery. In: Mariani G, Giuliano AE, Strauss HW (eds) Radioguided surgery – a comprehensive team approach. Springer, New York, pp 3–11
8. Goyal A, Newcombe RG, Mansel RE et al (2005) ALMANAC Trialists Group. Role of routine preoperative lymphoscintigraphy in sentinel node biopsy for breast cancer. Eur J Cancer 41:238–243
9. Even-Sapir E, Lerman H, Lievshitz G et al (2003) Lymphoscintigraphy for sentinel node mapping using a hybrid SPECT/CT system. J Nucl Med 44:1413–1420
10. Lerman H, Metser U, Lievshitz G et al (2006) Lymphoscintigraphic sentinel node identification in patients with breast cancer: the role of SPECTCT. Eur J Nucl Med Mol Imaging 33:329–337
11. Lerman H, Lievshitz G, Zak O et al (2007) Improved sentinel node identification by SPECT/CT in overweight patients with breast cancer. J Nucl Med 48:201–206
12. Zanzonico P, Heller S (2000) The intraoperative gamma probe: basic principles and choices available. Semin Nucl Med 1:33–48
13. Classe JM, Fiche M, Rousseau C et al (2005) Prospective comparison of 3 gamma-probes for sentinel lymph node detection in 200 breast cancer patients. J Nucl Med 46:395–399
14. Mariani G, Vaiano A, Nibale O, Rubello D (2005). Is the "ideal" gamma-probe for intraoperative radioguided surgery conceivable? J Nucl Med 46:388–390
15. Mathelin CE, Guyonnet JL (2006). Scintillation crystal or semiconductor gamma-probes: an open debate. J Nucl Med 47:373
16. Meller B, Sommer K, Gerl J et al (2006) High energy probe for detecting lymph node metastases with 18F-FDG in patients with head and neck cancer. Nuklearmedizin 45:153–159
17. Curtet C, Carlier T, Mirallié E et al (2007) Prospective comparison of two gamma probes for intraoperative detection of 18F-FDG: in vitro assessment and clinical evaluation in differentiated thyroid cancer patients with iodine-negative recurrence. Eur J Nucl Med Mol Imaging 34:1556–1562
18. Schneebaum S, Essner R, Even-Sapir E (2008) Positron-sensitive probes. In: Mariani G, Giuliano AE, Strauss HW (eds) Radioguided surgery – a comprehensive team approach. Springer, New York, pp 23–28
19. Huh SS, Rogers WL, Clinthorne NH (2007) An investigation of an intra-operative PET imaging probe. Nuclear Science Symposium Conference Record. NSS '07 IEEE pp 552–555
20. Manca G, Biggi E, Lorenzoni A et al (2011) Simultaneous detection of breast tumor resection margins and radioguided sentinel node biopsy using an intraoperative electronically collimated probe with variable energy window – a case report. Clin Nucl Med 36:e196–e198
21. Mariani G, Bruselli L, Kuwert T et al (2010). A review on the clinical uses of SPECT/CT. Eur J Nucl Med Mol Imaging 37:1959–1985
22. Vermeeren L, van der Ploeg IM, Valdés Olmos RA et al (2010) SPECT/CT for preoperative sentinel node localization. J Surg Oncol 101:184–190
23. Kobayashi K, Ramirez PT, Kim EE et al (2009) Sentinel node mapping in vulvovaginal melanoma using SPECT/CT lymphoscintigraphy. Clin Nucl Med 34:859–861
24. Leijte JA, van der Ploeg IM, Valdés Olmos RA et al (2009) Visualization of tumor blockage and rerouting of lymphatic drainage in penile cancer patients by use of SPECT/CT. J Nucl Med 50:364–367

25. van der Ploeg IM, Valdés Olmos RA, Kroon BB et al (2009) The yield of SPECT/CT for anatomical lymphatic mapping in patients with melanoma. Ann Surg Oncol 16:1537–1542
26. Vermeeren L, Valdés Olmos RA, Meinhardt W et al (2009) Value of SPECT/CT for detection and anatomic localization of sentinel lymph nodes before laparoscopic sentinel node lymphadenectomy in prostate carcinoma. J Nucl Med 50:865–870
27. Pandit-Taskar N, Gemignani ML, Lyall A et al (2010) Single photon emission computed tomography SPECT-CT improves sentinel node detection and localization in cervical and uterine malignancy. Gynecol Oncol 117:59–64
28. Vermeeren L, Meinhardt W, Valdes Olmos RA (2010) Prostatic lymphatic drainage with sentinel nodes at the ventral abdominal wall visualized with SPECT/CT: a case series. Clin Nucl Med 35:71–73
29. Vermeeren L, Valdés Olmos RA, Klop WM et al (2011) SPECT/CT for sentinel lymph node mapping in head and neck melanoma. Head Neck 33:1–6
30. Buscombe J, Paganelli G, Burak ZE et al; European Association of Nuclear Medicine Oncology Committee and Dosimetry Committee (2007) Sentinel node in breast cancer procedural guidelines. Eur J Nucl Med Mol Imaging 34:2154–2159
31. Cox CE, Cox JM, Mariani G et al (2008) Sentinel lymph node biopsy in patients with breast cancer. In: Mariani G, Giuliano AE, Strauss HW (eds) Radioguided surgery – a comprehensive team approach. Springer, New York, pp 87–97
32. Estourgie SH, Nieweg OE, Valdés Olmos RA et al (2003) Eight fals negative sentinel lymph node procedures in breast cancer: what went wrong? Eur J Surg Oncol 29:336–340
33. Leijte J, van der Ploeg IM, Valdés Olmos RA et al (2009) Visualization of tumor blockage and rerouting of lymphatic drainage in penile cancer patients by use of SPECT/CT. J Nucl Med 50:364–367
34. Varghese P, Abdel-Rahman AT, Akberali S et al (2008) Methylene blue dye – a safe and effective alternative for sentinel lymph node localization. Breast J 14:61–67
35. Rodier JF, Velten M, Wilt M et al (2007) Prospective multicentric randomized study comparing periareolar and peritumoral injection of radiotracer and blue dye for the detection of sentinel lymph node in breast sparing procedures: FRANSENODE trial. J Clin Oncol 25:3664–3669
36. Valdés Olmos RA, Vidal-Sicart S, Nieweg OE (2009) SPECT-CT and real-time intraoperative imaging: new tools for sentinel node localization and radioguided surgery? Eur J Nucl Med Mol Imaging 36:1–5
37. Vermeeren L, Valdés Olmos RA, Meinhardt W et al (2009) Intraoperative radioguidance with a portable gamma camera: a novel technique for laparoscopic sentinel node localisation in urological malignancies. Eur J Nucl Med Mol Imaging 36:1029–1036
38. Hoffman EJ, Tornai MP, Janecek M et al (1999) Intra-operative probes and imaging probes. Eur J Nucl Med 26:913–935
39. Scopinaro F, Tofani A, di Santo G et al (2008) High-resolution, hand-held camera for sentinel-node detection. Cancer Biother Radiopharm 23:43–52
40. Mathelin C, Salvador S, Huss D, Guyonnet JL (2007) Precise localization of sentinel lymph nodes and estimation of their depth using a prototype intraoperative mini gamma-camera in patients with breast cancer. J Nucl Med 48:623–629
41. Zaknun JJ, Giammarile F, Valeds-Olmos RA et al (2012) Changing paradigms in radioguided surgery and intraoperative imaging: the GOSTT concept. Eur J Nucl Med Mol Imaging 39:1
42. Vermeeren L, Klop WM, van den Brekel MW et al (2009) Sentinel node detection in head and neck malignancies: innovations in radioguided surgery. J Oncol 2009:681746
43. Duch J (2011) Portable gamma cameras: the real value of an additional view in the operating theatre. Eur J Nucl Med Mol Imaging 38:633–635
44. Vidal-Sicart S, Paredes P, Zanón G et al (2010) Added value of intraoperative real-time imaging in searches for difficult-to-locate sentinel nodes. J Nucl Med 51:1219–1225
45. Cardona-Arboniés J, Mucientes-Rasilla J, Moreno Elola-Olaso A et al (2012) Contribution of the portable gamma camera to detect the sentinel node in breast cancer during surgery. Rev Esp Med Nucl 31:130–134
46. Vidal-Sicart S, Brouwer OR, Valdés-Olmos RA (2011) Evaluation of the sentinel lymph node combining SPECT/CT with the planar image and its importance for the surgical act. Rev Esp Med Nucl 30:331–337
47. Vidal-Sicart S, Vermeeren L, Solà O, Valdés-Olmos RA (2011) The use of a portable gamma camera for preoperative lymphatic mapping: a comparison with a conventional gamma camera. Eur J Nucl Med Mol Imaging 38:636–641
48. Wendler T, Herrmann K, Schnelzer A et al (2010). First demonsriegertration of 3-D lymphatic mapping in breast cancer using freehand SPECT. Eur J Nucl Med Mol Imaging 37:1452–1461
49. Rieger A, Saeckl J, Belloni B et al (2011) First experiences with navigated radio-guided surgery using freehand SPECT. Case Rep Oncol 4:420–425
50. van der Poel HG, Buckle T, Brouwer OR et al (2011) Intraoperative laparoscopic fluorescence guidance to the sentinel lymph node in prostate cancer patients: clinical proof of concept of an integrated functional imaging approach using a multimodal tracer. Eur Urol 60:826–833
51. Keereweer S, Kerrebijn JD, van Driel PB et al (2011) Optical image-guided surgery – where do we stand? Mol Imaging Biol 13:199–207
52. Polom K, Murawa D, Rho YS et al (2011) Current trends and emerging future of indocyanine green usage in surgery and oncology: a literature review. Cancer 117:4812–4822